Comparison of Source Apportionment and Source Sensitivity of Ozone in a Three-Dimensional Air Quality Model

ARTICLE *in* ENVIRONMENTAL SCIENCE AND TECHNOLOGY · JULY 2002

Impact Factor: 5.33 · DOI: 10.1021/es011418f · Source: PubMed

4 AUTHORS, INCLUDING:

Alan M. Dunker
A.M. Dunker, LLC
37 PUBLICATIONS **1,259** CITATIONS

SEE PROFILE

Jerome P. Ortmann
General Motors Company
4 PUBLICATIONS **211** CITATIONS

SEE PROFILE

Environ. Sci. Technol. **2002**, *36,* 2953−2964

Comparison of Source Apportionment and Source Sensitivity of Ozone in a Three-Dimensional Air Quality Model

ALAN M. DUNKER*

Chemical and Environmental Sciences Laboratory, General Motors Research and Development Center, Warren, Michigan 48090-9055

GREG YARWOOD

ENVIRON International Corp., Novato, California 94945-5010

JEROME P. ORTMANN

Chemical and Environmental Sciences Laboratory, General Motors Research and Development Center, Warren, Michigan 48090-9055

GARY M. WILSON

ENVIRON International Corp., Novato, California 94945-5010

The ozone source apportionment technology (OSAT) estimates the contributions of different sources to ozone concentrations using a set of tracers for NO_x, total VOCs, and ozone and an indicator that ascribes instantaneous ozone production to NO_x or VOCs. These source contributions were compared to first-order sensitivities obtained by the decoupled direct method (DDM) for a three-dimensional simulation of an ozone episode in the Lake Michigan region. The cut-point for the OSAT indicator between VOC- and NO_x-sensitive ozone production agrees well with the DDM sensitivities to VOC and NO_x. In a ranking of the most important contributors to ozone concentrations >80 ppb, the OSAT and DDM results agreed on four of the top five contributors on average. The spatial distributions of the sensitivities and source contributions are similar, and the OSAT and DDM results for ozone >80 ppb correlate well. However, the source contributions ascribe substantially less relative importance to anthropogenic emissions and greater relative importance to the boundary concentrations than do the sensitivities. In regions where NO_x inhibits ozone formation and the sensitivity is negative, the source contribution is small and positive. For the same subdivision of the emissions, the OSAT is 14 times faster than the DDM, but the DDM has greater flexibility in defining which emissions to include and generates results for species other than ozone. The first-order sensitivities explain, on average, 70% of the ozone concentrations.

Introduction

To design strategies for reducing pollutant concentrations, it is very useful to know which emission sources are the most important. Ideally, one can quantitatively apportion the pollutant concentration at a particular location and time to all the emission sources that contribute. Such a process, often called source apportionment, is complicated for ozone because ozone is a secondary pollutant formed by nonlinear chemical reactions involving volatile organic compounds (VOCs) and nitrogen oxides (NO_x). The simplest approach to apportioning ozone in air quality modeling is to conduct simulations with and without the VOC and NO_x emissions from a given source so that the difference in ozone concentration between the two simulations is a measure of the source contribution (*1*).

There are, however, two limitations to all approaches to source apportionment of ozone. First, a source apportionment is not unique. In the case of the source-removal approach, the ozone changes depend on the order in which the sources are removed. Thus, to apportion the total ozone when there are three emission sources, we might remove source A, then B, and last C, ascribing the ozone change for each removal to the contribution of that source. However, removing the sources in the order C, A, B would give a different ozone change for each source because the ozone production from a given amount of emissions depends on what other emissions are present. Second, the source contribution represents the ozone produced from all of the source's emissions, but scaling this contribution to represent the ozone produced from a fraction of the emissions may not be accurate (e.g., a simulation of a 50% reduction in emissions from a source may yield an ozone change that is different from 50% of the source contribution, due to the nonlinear processes, such as chemistry).

Sensitivity coefficients describe the response of ozone and other species concentrations to changes in model inputs, including emissions. For three-dimensional (3D) models, only the first-order sensitivities have been calculated to date (*2*−*4*), and these describe the linear response to input changes. The major limitation of first-order sensitivities is that they may not adequately describe the ozone response if the magnitude of the emission changes becomes large. This is again a manifestation of the nonlinear chemistry involved in ozone formation.

While source apportionment and sensitivity analysis are different tools that calculate different quantities, they do both provide information on the relative importance of emission sources, initial concentrations (ICs), and boundary concentrations (BCs). The purpose of this paper is to compare results from one method for source apportionment, the ozone source apportionment technology (OSAT) (*5*, *6*), with first-order sensitivity coefficients obtained by the decoupled direct method (DDM) (*2*). A separate paper presents how sensitivities are calculated using the DDM and shows that the DDM is a very accurate method (*4*). Both the OSAT and the DDM have been implemented in the comprehensive air quality model with extensions (CAMx) (*6*−*8*). Having both tools in the same model allows for a consistent comparison between them, uncomplicated by the differences between air quality models.

In the next section, we give an overview of OSAT. This is an approach to source apportionment that takes into account transport, chemistry, and whether ozone formation is VOC- or NO_x-sensitive. A detailed description of the development and testing of OSAT is contained in refs *5* and *6*. We then describe the sensitivity coefficients briefly and how we can compare them to source contributions. For the comparison of OSAT and DDM, we applied CAMx to an ozone episode in the Lake Michigan region. We compare the ranking of importance, the magnitude, and the spatial distribution of

* Corresponding author phone: (586) 986-1625; fax: (586) 986-1910; e-mail: alan.m.dunker@gm.com.

10.1021/es011418f CCC: $22.00
Published on Web 05/23/2002

the source contributions with analogous results from the sensitivities. A comparison of the efficiency of OSAT and DDM is also given.

Methodology

Ozone Source Apportionment Technology. Photochemical grid models simulate ozone formation by representing species concentrations on a 3D grid and advancing the concentrations in time by approximating the effects of atmospheric processes. The concentration of an ozone precursor in a grid cell represents the total concentration from all sources because the chemical reactions are dependent on the total concentration. Consequently, the contributions of the individual sources are indistinguishable within the model.

OSAT was designed as an addition to an air quality model with several objectives in mind. First, the source−receptor relationships should be consistent with the formulation and predictions of the host model. Second, the presence of OSAT should not change the predictions of the model. Third, OSAT must be efficient in order to track ozone contributions from many separate sources. We summarize here the implementation of OSAT for CAMx, but, because all grid models are conceptually similar, OSAT can be applied to other models.

OSAT employs tracers to follow ozone precursors from their point of release through the 3D modeling domain. At the locations where ozone is formed, ozone tracers are created, with different ozone tracers representing the contributions from different sources of precursors. Then, OSAT tracks the movement of the ozone tracers. The conceptual challenges result from the complexity of the chemical relationships between ozone and precursors, with respect both to ozone formation and precursor destruction. The intent is to develop a simple scheme that captures the essence of these chemical relationships and thus has descriptive power to explain the model results. To maintain simplicity, OSAT requires various assumptions. The most important assumptions relate to allocating ozone changes among different sources and between VOC and NO_x precursors.

The OSAT approach is to add families of tracers to the model simulation, one family for each source group i, $i = 1, \ldots, m$. Each family contains four tracers: N_i, the tracer for NO_x from source group i; V_i, the tracer for VOCs from source group i; $O3N_i$, the tracer for ozone formed from NO_x from source group i; and $O3V_i$, the tracer for ozone formed from VOCs from source group i. OSAT is designed to apportion all of the predicted ozone concentration at any location and time so that the sums of the tracers satisfy the following equalities:

$$\sum_{i=1}^{m} N_i = NO + NO_2 \quad (1)$$

$$\sum_{i=1}^{m} V_i = \sum_{j=1}^{n_V} VOC_j \quad (2)$$

$$\sum_{i=1}^{m} O3N_i + \sum_{i=1}^{m} O3V_i = O_3 \quad (3)$$

where n_V is the number of VOCs in the chemical mechanism, and NO, NO_2, VOC_j, and O_3 are the concentrations of these species predicted by the model.

To satisfy eqs 1−3, tracers must be included for all sources of precursors and ozone, namely, all the emissions, ICs, and BCs. For emissions, the source groups are defined on the basis of source category (e.g., point-source emissions) and/or geographic area. The V_i tracers are defined as containing a single carbon atom and so have an emission rate equal to the sum of the VOC emissions in moles of carbon. The emission rate for N_i is set equal to the NO_x emission rate. The tracers for the ICs are set equal to the VOC or NO_x ICs and receive no more mass input after the start of the simulation. The tracers for the BCs track the fluxes of VOC and NO_x entering the model from the lateral and top boundaries. The ICs and BCs also introduce ozone directly into the model. Because there is no way of determining whether this ozone was formed under VOC- or NO_x-sensitive conditions, this ozone is apportioned equally to the $O3V_i$ and $O3N_i$ tracers. However, subsequent ozone formation within the model domain from initial and boundary VOCs and NO_x is allocated to $O3V_i$ and $O3N_i$ tracers based on whether the ozone formed under VOC- or NO_x-sensitive conditions.

Each tracer deposition velocity at the lower boundary must correspond to the species that the tracer represents. Thus, the deposition velocity for the $O3V_i$ and $O3N_i$ tracers is set equal to the ozone deposition velocity. The deposition velocity for each tracer, N_i, is set equal to the concentration-weighted average of the deposition velocities for NO and NO_2. Similarly, the deposition velocity for each tracer V_i is set equal to the concentration-weighted average of the deposition velocities for the individual VOCs (with the weighting performed on a mol of carbon basis).

The algorithms used to update the tracer concentrations in the model must maintain consistency between the tracers and the chemical species. For example, consider a species S that is represented by a sum of m tracer species, s_i: $S = \sum_{i=1}^{m} s_i$. The concentration of S is advanced across a time step Δt by a model algorithm, F

$$S(t + \Delta t) = F(S[t])$$

The tracer concentrations must be advanced by a corresponding algorithm, f

$$s_i(t + \Delta t) = f(s_i[t])$$

If the algorithm F has a linear response to the concentration S, then

$$S(t + \Delta t) = F\left(\sum_{i=1}^{m} s_i[t]\right) = \sum_{i=1}^{m} F(s_i[t])$$

and the algorithms F and f are the same. In CAMx, only the horizontal advection and chemical algorithms are nonlinear in the species concentrations. Therefore, the OSAT tracers can be advanced in time using the standard CAMx algorithms for all processes except horizontal advection and chemistry.

The basic equation for horizontal advection is linear in the species concentration. However, the numerical algorithms used in CAMx (*9*−*11*) to solve the horizontal advection equation are nonlinear in the concentration due to the procedures employed to counteract artificial (or numerical) diffusion. These algorithms can be expressed as a two-step process: (1) calculate species fluxes between adjacent grid cells based on the wind velocity and the concentration distribution; and (2) update the concentration distribution using the calculated fluxes in a linear step that is the same for each advection algorithm. This presents a simple approach to solving horizontal advection for the OSAT tracers; namely, the tracers are advected using the fluxes calculated for the corresponding chemical species. Thus, the fluxes calculated for ozone in step 1 are used to advect ozone and also the $O3V_i$ and $O3N_i$ tracers in step 2. This approach maintains consistency between the OSAT tracers and the chemical species and also improves efficiency by avoiding the need to separately calculate the advective fluxes for each OSAT tracer.

The requirements for the OSAT chemical algorithm are to decay the precursor tracers N_i and V_i and to allocate ozone production to the ozone tracers $O3N_i$ and $O3V_i$. We decay the N_i tracer mass in each grid cell at each time step according to the chemical change in NO_x, ΔNO_x, weighted by the tracer contribution to the total of the NO_x tracers from all source groups:

$$N_i(t + \Delta t) = N_i(t) + \Delta NO_x \times N_i(t) / \sum_{i=1}^{m} N_i(t) \quad (4)$$

Similarly, we decay the V_i tracer mass in each grid cell at each time step according to the chemical change in total VOCs, ΔVOC, weighted by the tracer contribution to the total of all the VOC tracers. However, because the reactivity of VOCs from different source groups can be different, a weighting factor based on the OH reactivity of each VOC tracer, $k\mathrm{OH}_i$, is also introduced. The $k\mathrm{OH}_i$ for each source group is calculated by averaging the OH rate constants of the speciated VOC emissions for each source group. (This averaging is done separately for each day of the simulation.) Thus, we use the equation

$$V_i(t + \Delta t) = V_i(t) + \Delta\mathrm{VOC} \times V_i(t) \times k\mathrm{OH}_i / \sum_{i=1}^{m} [V_i(t) \times k\mathrm{OH}_i] \quad (5)$$

The $O3N_i$ and $O3V_i$ tracers for each source group accumulate a weighted fraction of the net ozone change, ΔO_3, that occurs in each grid cell at each time step. We apportion ΔO_3 to the tracers in three steps. First, if there is local (grid cell/time step) net ozone production, we determine whether the production is NO_x- or VOC- sensitive (described next). Second, for ozone production under NO_x-sensitive conditions, we allocate ΔO_3 to the $O3N_i$ tracers according to the proportionate contribution of the tracers

$$O3N_i(t + \Delta t) = O3N_i(t) + \Delta O3 \times N_i(t) / \sum_{i=1}^{m} N_i(t) \quad (6)$$

If the ozone production is VOC-sensitive, we allocate ΔO_3 to the $O3V_i$ tracers according to

$$O3V_i(t + \Delta t) = O3V_i(t) + \Delta O3 \times V_i(t) \times k\mathrm{OH}_i / \sum_{i=1}^{m} [V_i(t) \times k\mathrm{OH}_i] \quad (7)$$

Third, if there is net ozone destruction rather than production, we allocate ΔO_3 across all the ozone tracers using

$$O3N_i(t + \Delta t) = O3N_i(t) + \Delta O3 \times O3N_i(t) / \sum_{i=1}^{m} [O3N_i(t) + O3V_i(t)] \quad (8)$$

and an analogous equation for $O3V_i$.

To determine whether to apply eq 6 or 7, OSAT requires an indicator of the instantaneous sensitivity of ozone to VOC and NO_x levels present in a grid cell. This instantaneous sensitivity is reflected in the fate of radicals because reactions of peroxy radicals (HO_2, RO_2) with NO are the driver for ozone production. Because radicals are interconverted rapidly, the sum of OH, HO_2, and RO_2 radicals is often treated as the odd-hydrogen radical pool, HO_x. When NO_x is plentiful, the main HO_x removal pathway is nitric acid formation

$$OH + NO_2 (+M) \rightarrow HNO_3 (+M)$$

Under these conditions, ozone formation is limited by the rate at which new radicals can be formed, which is the VOC-sensitive condition. Thus, nitric acid production is indicative of VOC-sensitive ozone formation.

When NO_x is scarce, radical−radical reactions dominate HO_x removal, for example,

$$HO_2 + HO_2 (+M) \rightarrow H_2O_2 + O_2 (+M)$$

$$HO_2 + RO_2 \rightarrow ROOH + O_2$$

Ozone formation is limited by the availability of NO to react with HO_2 and RO_2 radicals, which is the NO_x-sensitive condition. The HO_2 and RO_2 radicals that do not react with NO participate in peroxide formation; thus, peroxide production is indicative of NO_x-sensitive ozone formation.

Sillman (*12*) developed indicators of VOC- versus NO_x-sensitive ozone formation based on the ratio of peroxide production to nitric acid production and proposed that the transition or cut-point between these conditions occurs when

$$(P_{H_2O_2} + P_{ROOH}) / P_{HNO_3} = 0.5 \quad (9)$$

The production rates of nitric acid, P_{HNO_3}, and hydrogen peroxide, $P_{H_2O_2}$, in each grid cell at each time step are readily accessible. However, the production rate of organic peroxides, P_{ROOH}, may not be accessible because some chemical mechanisms do not explicitly track organic peroxides. The balance between P_{ROOH} and $P_{H_2O_2}$ depends on the relative production of HO_2 and RO_2 radicals, but Sillman found that it is not highly variable within/across simulations. Accordingly, he proposed that eq 9 is equivalent to a cut-point of

$$P_{H_2O_2} / P_{HNO_3} = 0.35 \quad (10)$$

Hence, when this ratio exceeds 0.35, we define ozone formation to be NO_x-sensitive and employ eq 6. When this ratio is less than 0.35, we define ozone formation to be VOC-sensitive and use eq 7.

Sensitivity Coefficients. The first-order sensitivity coefficient is the partial derivative of the concentration of the pth species at some spatial location x, y, z and time t, with respect to a parameter λ in the model, $\partial c_p(x, y, z, t; \lambda)/\partial\lambda$. For this work, we define an array of parameters $\underline{\lambda}$, consisting of λ_j, $j = 1, \ldots, M$, that scales all of the emissions, ICs, and BCs according to the equation

$$I_j(x, y, z, t; \lambda_j) = (1 + \lambda_j) \times I_{j0}(x, y, z, t) \quad (11)$$

Here, I_{j0} is the original jth input to the model, for example, NO_x emissions from point sources in a specific geographic region, and I_j is the scaled input. The number of parameters, M, depends on how finely or coarsely one subdivides the model inputs.

We have calculated the sensitivities to the λ_j using the DDM, as described in detail elsewhere (*2*, *4*). Briefly, the 3D model begins with a set of governing differential equations. These differential equations are then converted to a set of finite difference equations by application of various numerical algorithms and selection of a grid of spatial points and a sequence of times. In the DDM, we differentiate the finite difference equations representing the model with respect to the parameters λ_j, thus creating an auxiliary set of finite difference equations for the sensitivities. We solve this auxiliary set of equations in parallel with the model equations.

In OSAT, CO emissions are not included as part of VOC emissions, but the O_3 formed from CO is very likely allocated to the VOC emissions. To maintain consistency and include this source of O_3, we include CO as part of VOC when calculating sensitivities with respect to VOC emissions.

The concentration c_p can be expanded in a Taylor series in the array of parameters $\underline{\lambda}$.

$$c_p(x, y, z, t; \underline{\lambda}) = c_p(x, y, z, t; \underline{\lambda} = 0) + \sum_{i=1}^{M} \frac{\partial c_p}{\partial \lambda_i}\bigg|_{\underline{\lambda}=0} \lambda_i + \frac{1}{2}\sum_{i=1}^{M}\sum_{j=1}^{M} \frac{\partial^2 c_p}{\partial \lambda_i\, \partial \lambda_j}\bigg|_{\underline{\lambda}=0} \lambda_i\, \lambda_j + \ldots$$

This is an expansion about $\underline{\lambda} = 0$ (i.e., the original emissions, ICs, and BCs) (eq 11). We may project to zero emissions, ICs, and BCs by setting $\underline{\lambda} = -1$. Also, it is intuitively obvious and can be shown mathematically that, if the emissions, ICs, and BCs for all species in the model are zero, the ozone concentration $c_p(x, y, z, t; \underline{\lambda} = -1)$ is zero. This leads to the equation

$$c_p(x, y, z, t; \underline{\lambda} = 0) = \sum_{i=1}^{M} \frac{\partial c_p}{\partial \lambda_i}\bigg|_{\underline{\lambda}=0} - \frac{1}{2}\sum_{i=1}^{M}\sum_{j=1}^{M} \frac{\partial^2 c_p}{\partial \lambda_i\, \partial \lambda_j}\bigg|_{\underline{\lambda}=0} + \ldots \quad (12)$$

which relates $c_p(x, y, z, t; \underline{\lambda} = 0)$, the concentration predicted with the original emissions, ICs, and BCs, to the sensitivities alone. This equation suggests a connection between sensitivity coefficients and source apportionment. If the second- and higher-order sensitivities (second- and higher-order derivatives) are small, then the first-order sensitivities provide an approximate allocation of the ozone concentration at a particular location and time to the set of M emissions, ICs, and BCs. Conversely, if the ozone concentration is allocated to the M model inputs by OSAT or some other technique, eq 12 indicates that the individual source contributions will contain contributions from all orders of sensitivities. Equation 12 also shows that a measure of the importance of the second- and higher-order sensitivities can be obtained by comparing the sum of all of the first-order sensitivities to the concentration c_p.

Simulations. We simulated the ozone episode of July 7−13, 1995, in the Lake Michigan region using the same model configuration, meteorological inputs, emissions and ICs and BCs as in our work to implement and test the DDM (*4*). Briefly, we used the Bott algorithm (*11*) for advection and the Carbon Bond IV (CB IV) chemical mechanism (*13*) with updated radical termination and isoprene reactions (*14*). The horizontal modeling domain (Figure 1) contains a coarse grid of 58 × 93 cells, each cell being approximately 12 km × 12 km. There is also a fine grid of 81 × 120 cells nested within the coarse grid and centered on the southern end of Lake Michigan, with each of these cells being approximately 4 km × 4 km. Both grids have seven vertical layers. We used the coarse grid for the initialization days, July 7−9, and both coarse and fine grids on July 10−13. We took the various model inputs from previous work in simulating this episode (*15*). A summary of the emissions and the CAMx predictions for ozone on July 13 are contained in the paper on the DDM (*4*).

We divided the modeling domain into the 13 source regions shown in Figure 1 and tracked emissions from each region separately. In addition, we divided the emissions within each source region into three categories: biogenic sources, anthropogenic area sources, and point sources. The contributions to ozone from the ICs and the east, west, south, north, and top BCs were also tracked separately. Last, contributions from VOCs and NO_x were always tracked separately. This yields a total of 90 individual contributions to the ozone concentration (13 × 3 × 2 + 6 × 2). These contributions were calculated in OSAT using 180 VOC, NO_x, and ozone tracers. For the DDM, we divided the inputs in the same manner except that the ozone in the ICs and BCs was tracked separately from VOC and NO_x. Hence, we calculated a total of 96 sensitivities (13 × 3 × 2 + 6 × 3).

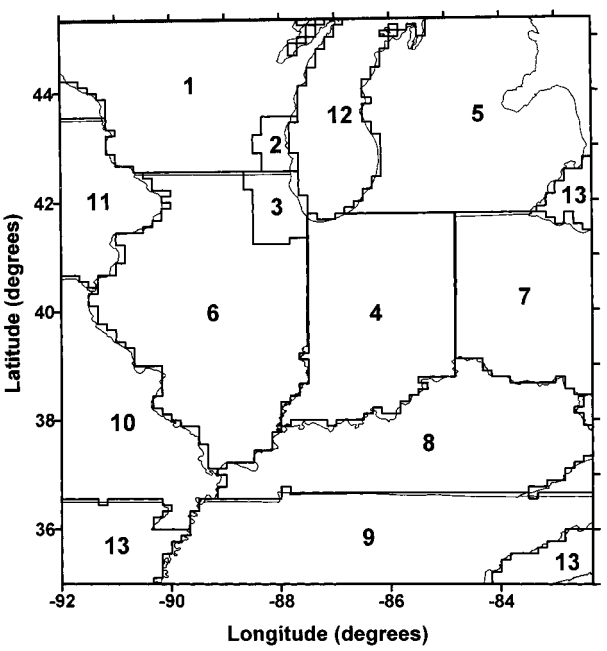

FIGURE 1. Subdivision of the modeling domain into 13 source regions, which are shown by the heavier line segments. Source region 13 consists of all areas along the boundaries that are not included in regions 1−12.

When comparing to OSAT results for BCs, we adjusted the sensitivity to BC VOC by adding 50% of the sensitivity to BC ozone. Thus, $[\partial O_3/\partial \text{BC VOC}]_{\text{adjusted}} = \partial O_3/\partial \text{BC VOC} + 0.5\partial O_3/\partial \text{BC } O_3$. Similarly, we adjusted the sensitivity to BC NO_x by adding 50% of the sensitivity to BC ozone. We also adjusted the sensitivity to IC VOC and NO_x by an analogous procedure. These adjustments mirror the approach in OSAT, whereby the BC or IC ozone is allocated equally to the corresponding O3V and O3N tracers.

To compare results from OSAT and DDM, we selected six receptor regions that span a range of conditions (see Figure 2). Regions 1 and 3 have low to moderate emissions but are sometimes downwind of the large emissions in the Chicago area. Region 2 has essentially no emissions but is usually downwind of the emissions in the Chicago area. Regions 4 and 5 contain the emissions of Chicago and Gary, Indiana, respectively. Region 6 has primarily rural emissions but can be downwind of emissions from St. Louis or point sources in the Ohio River Valley.

Results and Discussion

Evaluation of the Indicator Ratio for OSAT. By having both the DDM and OSAT in the same model, we were able to evaluate how well the $P_{H_2O_2}/P_{HNO_3}$ indicator ratio performs in OSAT for apportioning ozone to VOC and NO_x. The questions considered are whether the cut-point of 0.35 is appropriate and how sensitive the OSAT results are to this assumption. We analyzed information from individual grid cells and time steps throughout the first 3 days of the simulation, July 7−9, 1995, sampling cells randomly to reduce the amount of data. Sampling 2% of the cells during daylight hours resulted in about 100 000 cells and time steps for each day. For each cell and time step, we recorded the $P_{H_2O_2}/P_{HNO_3}$ ratio, the ozone production, and the sensitivities of ozone at the end of the time step to the VOC and NO_x concentrations at the beginning of the time step, calculated using the DDM. (These sensitivities to concentrations at the beginning of a time step are different from and were calculated separately

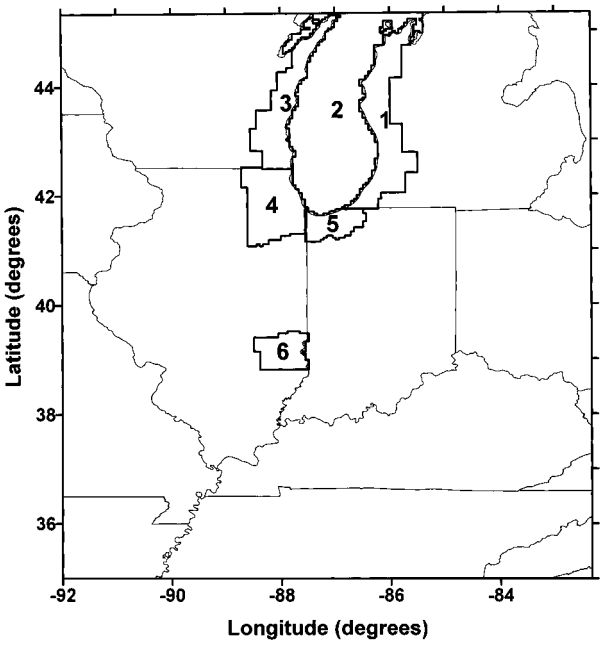

FIGURE 2. Locations of the six receptor regions.

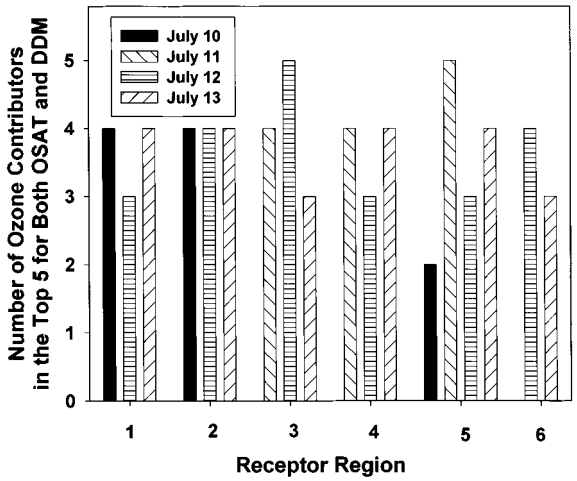

FIGURE 3. Agreement between OSAT and DDM for the top five contributors to ozone concentrations at 1500−1600 CST. OSAT and DDM results are averaged over grid cells in the receptor regions with ozone > 80 ppb. Missing bars are cases in which ozone is < 80 ppb throughout the region.

from the sensitivities to emissions, ICs, and BCs defined by eqs 11 and 12.) The sensitivities were used to divide the ozone production into VOC- and NO_x-sensitive portions by defining

$$F_{\mathrm{VOC}} = \left[\frac{\partial \mathrm{O_3}}{\partial \mathrm{VOC}} + \left|\frac{\partial \mathrm{O_3}}{\partial \mathrm{VOC}}\right|\right] \Bigg/ \left[\frac{\partial \mathrm{O_3}}{\partial \mathrm{VOC}} + \left|\frac{\partial \mathrm{O_3}}{\partial \mathrm{VOC}}\right| + \frac{\partial \mathrm{O_3}}{\partial \mathrm{NO}_x} + \left|\frac{\partial \mathrm{O_3}}{\partial \mathrm{NO}_x}\right|\right] \quad (13)$$

to be the VOC-sensitive fraction and an analogous ratio to be the NO_x-sensitive fraction. We used the definition in eq 13 because the sensitivity to NO_x (and occasionally to VOC) can be negative. In such cases, all ozone production is allocated to the species with the positive sensitivity. When both sensitivities are positive, ozone production is allocated in proportion to the VOC and NO_x sensitivities.

Table 1 presents the average VOC- and NO_x-sensitive ozone production for each day stratified according to the $P_{H_2O_2}/P_{HNO_3}$ indicator ratio. Ozone production is overwhelmingly VOC-sensitive at low indicator ratios (<0.15) and NO_x-sensitive at high indicator ratios (>1.0), with a transition region between 0.15 and 1.0. An equal split between VOC- and NO_x-sensitive ozone production occurs close to the indicator value of 0.35 previously proposed (*12*) as the cut-point between VOC- and NO_x-sensitive ozone production. Thus, these results support the use of 0.35 for the cut-point in OSAT. The results also show that the transition from VOC- to NO_x-sensitive ozone production is a progressive rather than discrete function of the indicator ratio. Moving the cut-point for the indicator ratio from the bottom to the top of the transition region (from 0.15 to 1.0) could affect the classification of 20−30% of the ozone production as VOC- or NO_x-sensitive in OSAT. Moving the cut-point within a more realistic range of between 0.25 and 0.5 would affect the classification of only 4−6% of the ozone production because relatively few cells have indicator ratios close to 0.35. This suggests that OSAT will not be very sensitive to uncertainties in the indicator ratio cut-point.

Comparison of Rankings. One use of source contributions and sensitivities is simply to rank the emissions, ICs, and BCs according to their importance for ozone in a particular receptor region. This provides information on which model inputs have the largest effects without attempting to relate changes in inputs to changes in ozone concentrations. In comparing the OSAT and DDM rankings, we focused on the highest ozone concentrations, which are of the most interest in designing control strategies. We first averaged the OSAT and DDM results over each receptor region, including only those grid cells with ozone > 80 ppb. (In this and our other

TABLE 1. Average Ozone Production Sensitive to VOC or NO_x and the Corresponding Values of the Indicator Ratio Used in OSAT[a]

	July 7, 1995			July 8, 1995			July 9, 1995		
indicator ratio[b]	NO_x-sensitive O_3 prod.[c]	VOC-sensitive O_3 prod.[c]	number of cells and time steps	NO_x-sensitive O_3 prod.[c]	VOC-sensitive O_3 prod.[c]	number of cells and time steps	NO_x-sensitive O_3 prod.[c]	VOC-sensitive O_3 prod.[c]	number of cells and time steps
<0.05	0.2	7.8	16449	0.4	11.9	11063	0.4	13.9	6821
0.05−0.10	0.2	12.5	3829	0.5	17.8	2523	0.8	20.8	1899
0.10−0.15	1.6	11.2	2670	2.6	16.5	1776	3.1	17.8	1367
0.15−0.25	4.1	8.7	3983	5.5	12.4	2637	6.5	14.2	2067
0.25−0.35	6.5	7.1	2885	8.1	9.2	2265	9.3	10.8	1629
0.35−0.50	8.1	5.7	3335	9.4	7.1	2878	9.9	7.5	2270
0.50−1.00	9.5	3.9	7244	11.6	5.1	6481	11.0	4.9	6162
1.00−5.00	9.1	1.7	17058	11.7	2.3	15922	13.2	2.4	18521
>5.00	3.0	0.2	49825	4.8	0.3	43756	6.4	0.3	50790

[a] Random sampling of 2% of cells during daylight hours. NO_x-sensitive and VOC-sensitive ozone production determined using DDM sensitivity coefficients (see eqn 13). [b] Ratio of production of H_2O_2 to production of HNO_3 over the time step, $P_{H_2O_2}/P_{HNO_3}$. Used in OSAT to apportion O_3 to VOC or NO_x. [c] Ozone production in pmol/m^3 per time step, averaged over cells and time steps.

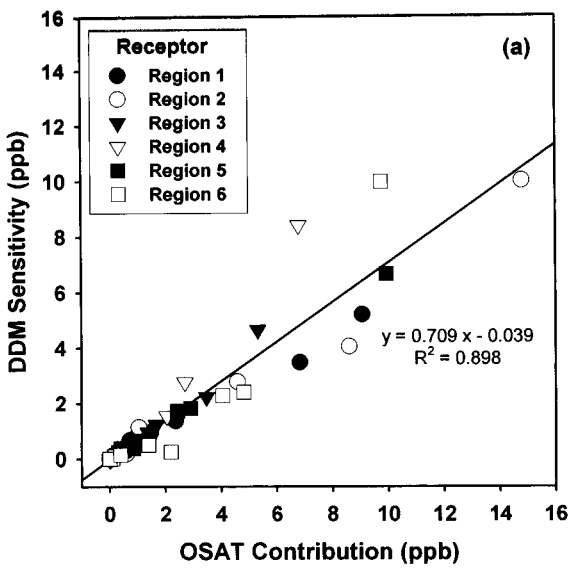
(a)
Receptor
Region 1
Region 2
Region 3
Region 4
Region 5
Region 6
y = 0.709 x - 0.039
R2 = 0.898
DDM Sensitivity (ppb)
OSAT Contribution (ppb)

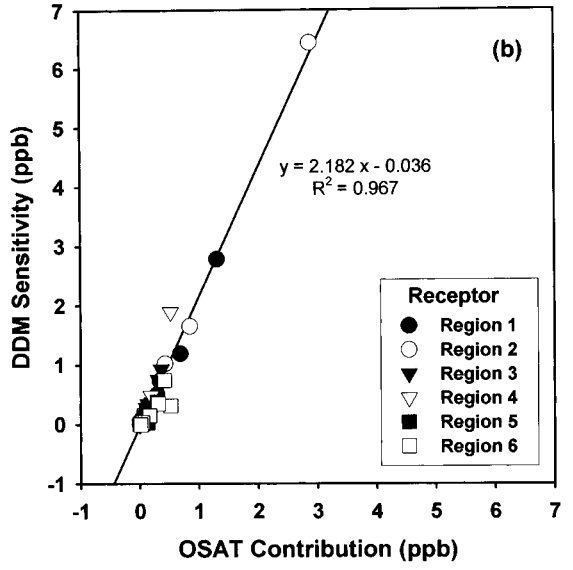
(b)
y = 2.182 x - 0.036
R2 = 0.967
Receptor
Region 1
Region 2
Region 3
Region 4
Region 5
Region 6
DDM Sensitivity (ppb)
OSAT Contribution (ppb)

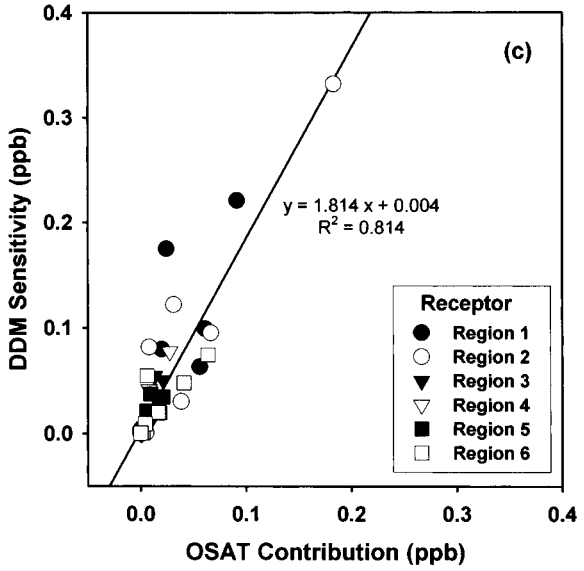
(c)
y = 1.814 x + 0.004
R2 = 0.814
Receptor
Region 1
Region 2
Region 3
Region 4
Region 5
Region 6
DDM Sensitivity (ppb)
OSAT Contribution (ppb)

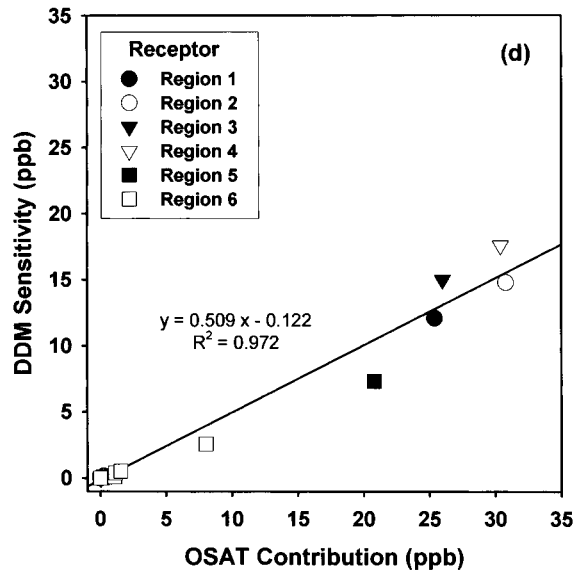
(d)
Receptor
Region 1
Region 2
Region 3
Region 4
Region 5
Region 6
y = 0.509 x - 0.122
R2 = 0.972
DDM Sensitivity (ppb)
OSAT Contribution (ppb)

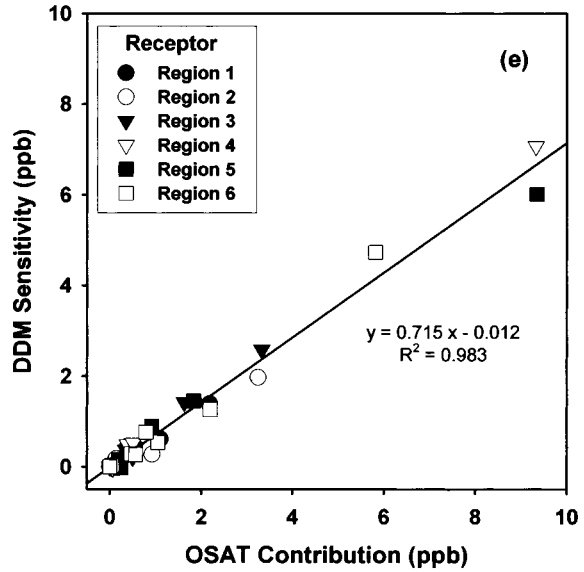
(e)
Receptor
Region 1
Region 2
Region 3
Region 4
Region 5
Region 6
y = 0.715 x - 0.012
R2 = 0.983
DDM Sensitivity (ppb)
OSAT Contribution (ppb)

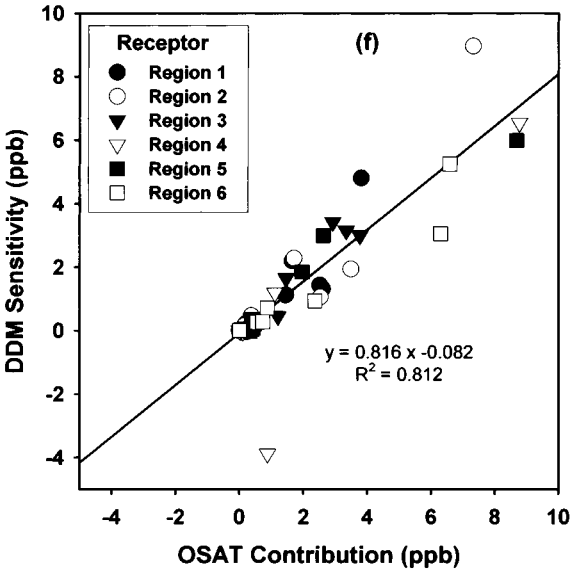
(f)
Receptor
Region 1
Region 2
Region 3
Region 4
Region 5
Region 6
y = 0.816 x -0.082
R2 = 0.812
DDM Sensitivity (ppb)
OSAT Contribution (ppb)

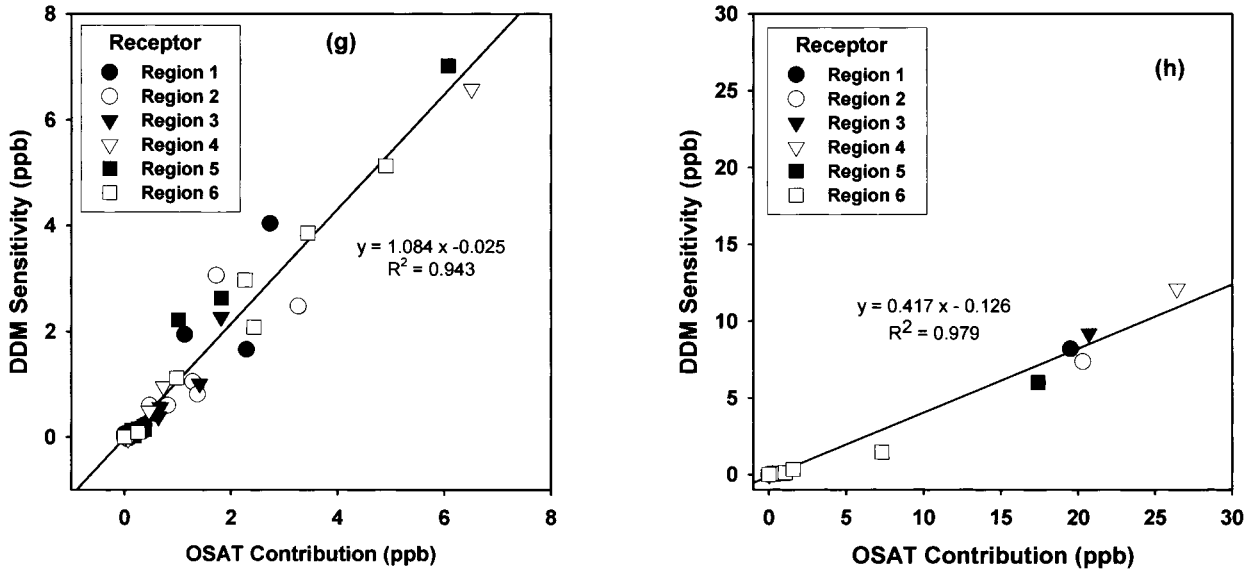

FIGURE 4. Comparison of sensitivities and source contributions for different emissions categories and boundary concentrations. OSAT and DDM results are averaged over grid cells in the receptor regions with ozone > 80 ppb on July 13, 1995, 1500−1600 CST. (a) biogenic VOC emissions; (b) anthropogenic area-source VOC emissions; (c) point-source VOC emissions; (d) lateral and top boundary VOC concentrations; (e) biogenic NO_x emissions; (f) anthropogenic area-source NO_x emissions; (g) point-source NO_x emissions; (h) lateral and top boundary NO_x concentrations.

analyses, we used results from the surface layer of the model.) Because the sensitivities can be positive or negative, we used the absolute value of the sensitivities to avoid cancellation in the averaging and to determine the most important sensitivities regardless of their sign. Next, we found the top five source contributions and top five sensitivities and determined how many agreed. Agreement was determined without regard to order among the top five. Thus, if biogenic VOC emissions from source region 6 were ranked first by OSAT and fourth by DDM, we counted this as agreement in that the contributor was in the top five in both rankings.

Figure 3 displays the agreement between the OSAT and DDM rankings for the top five contributors to ozone on July 10−13, 1500−1600 CST. (Results are missing for one or 2 days in receptor regions 1−4 and 6 because, on those days, ozone < 80 ppb for all cells in the regions.) Depending on the day and receptor region, the two rankings agree on two to five of the top five contributors, and on average the rankings agree on four of the top five contributors. Also, the level of agreement is about the same for all receptor regions. We conclude that OSAT and DDM agree reasonably well on the most important contributors to the highest ozone concentrations but disagree on about 20% of the important contributors.

Comparison of Values. Because of the definition of the parameters in eq 11 and the relationship in eq 12, it is possible to compare directly the values of the sensitivities and source contributions. The sensitivities have units of concentration, as do the source contributions, and an appropriate sum of the sensitivities of all orders is equal to the total ozone concentration. Figure 4 contains plots of the DDM sensitivity versus the OSAT source contribution averaged over the receptor regions on July 13, 1995, 1500−1600 CST. We focus again on the locations with the higher ozone concentrations, so the averaging includes only DDM and OSAT results for grid cells with ozone > 80 ppb. We segregated the comparisons according to the contributor to ozone. Thus, there are separate plots for the BCs and the three categories of emissions and for VOC and NO_x. There are a total of 78 points in the emissions plots, because there are 13 source regions for a given emissions category and six receptor regions. In the BC plots, there are 30 points (four lateral boundaries and a top boundary for each of six receptor regions). Both the DDM and OSAT results for the ICs are very small by the close of July 9; hence, no comparisons are shown for the ICs.

There is good correlation between the DDM sensitivities and OSAT source contributions for all of the cases in Figure 4, with R^2 values being greater than 0.8. The degree of correlation appears independent of the magnitude of the sensitivity or source contribution. For example, the correlation is the same for point-source VOC emissions and area-source NO_x emissions, Figure 4, parts c and f, though the sensitivities and source contributions for the former case are over an order of magnitude smaller than for the latter case. Similarly, there is equally high correlation in Figure 4, parts b and d, though a factor of 3−4 difference in magnitudes. Also, there is no obvious difference among the receptor regions in the correlation between the DDM and OSAT results. Generally, all of the sensitivities for these six receptor regions are positive or only slightly negative during 1500−1600 CST, the one exception being the sensitivity for receptor region 4 to area-source NO_x emissions from source region 3, as seen in Figure 4f. OSAT gives a small positive source contribution corresponding to this negative sensitivity coefficient.

While there is good correlation between the DDM and OSAT results, there is disagreement between the magnitudes of the two sets of results, as evidenced by the slope of the regression lines in Figure 4. The sensitivities ascribe greater importance (slope > 1.) to anthropogenic area-source VOC emissions and point-source VOC and NO_x emissions than do the OSAT source contributions. The OSAT results ascribe greater importance to biogenic VOC and NO_x emissions, anthropogenic area-source NO_x emissions, and VOC and NO_x BCs.

Some of this disagreement is due to an overall tendency of the sensitivities to be smaller than the source contributions. The sum of all the first-order sensitivities is 65−71% of the ozone concentration in the six receptor regions (when averaged over cells with ozone > 80 ppb). (See also additional results below.) However, the sum of the OSAT source contributions is always equal to the ozone concentration. Thus, we might expect that the regression slopes in Figure 4 would be in the range 0.65−0.71. Slopes outside this range

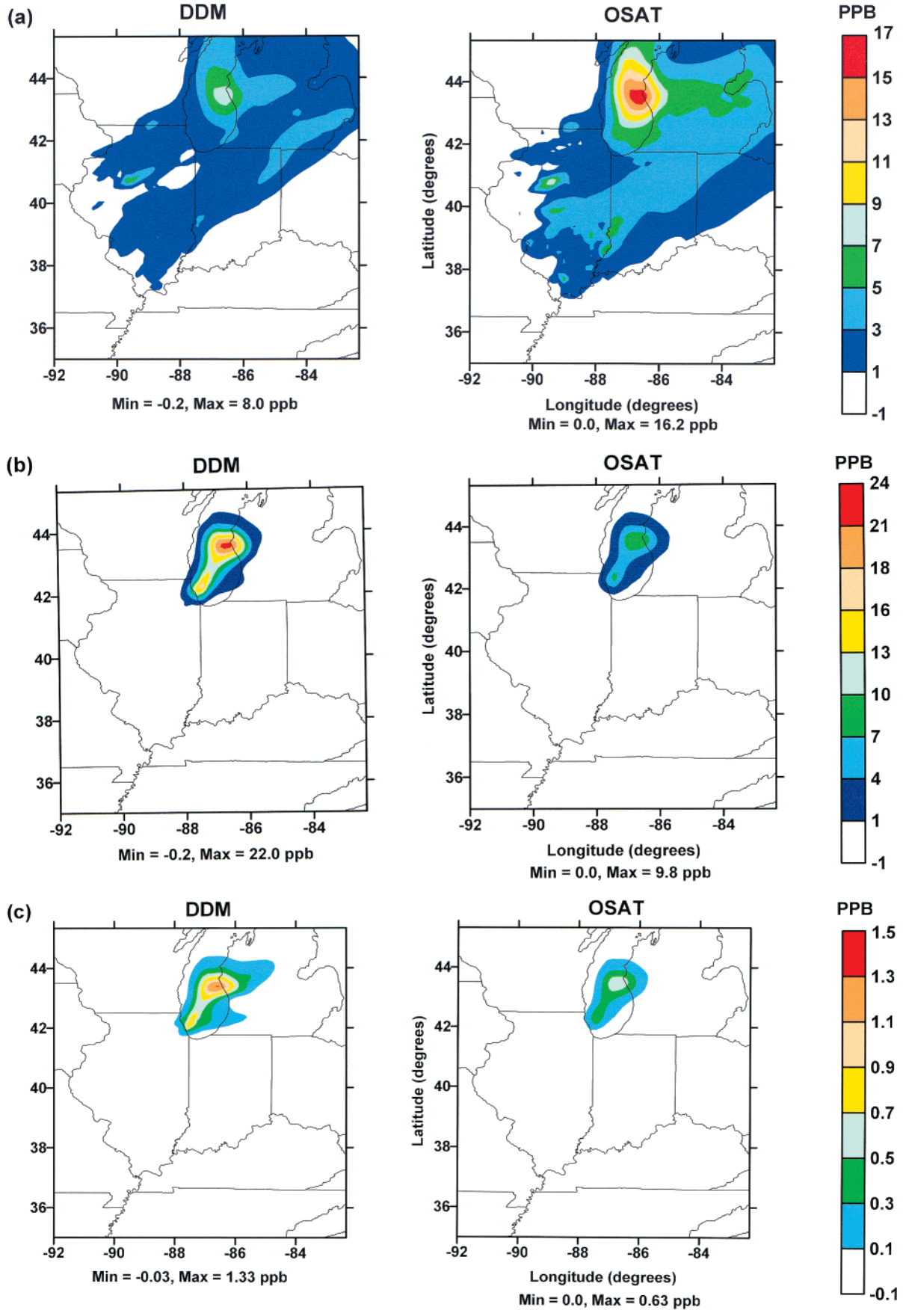

FIGURE 5. Comparison of the sensitivity (DDM) of ozone on July 13, 1995, 1500−1600 CST to emissions and the corresponding source contribution (OSAT). (a) biogenic VOC emissions from source region 6; (b) anthropogenic area-source VOC emissions from source region 3;

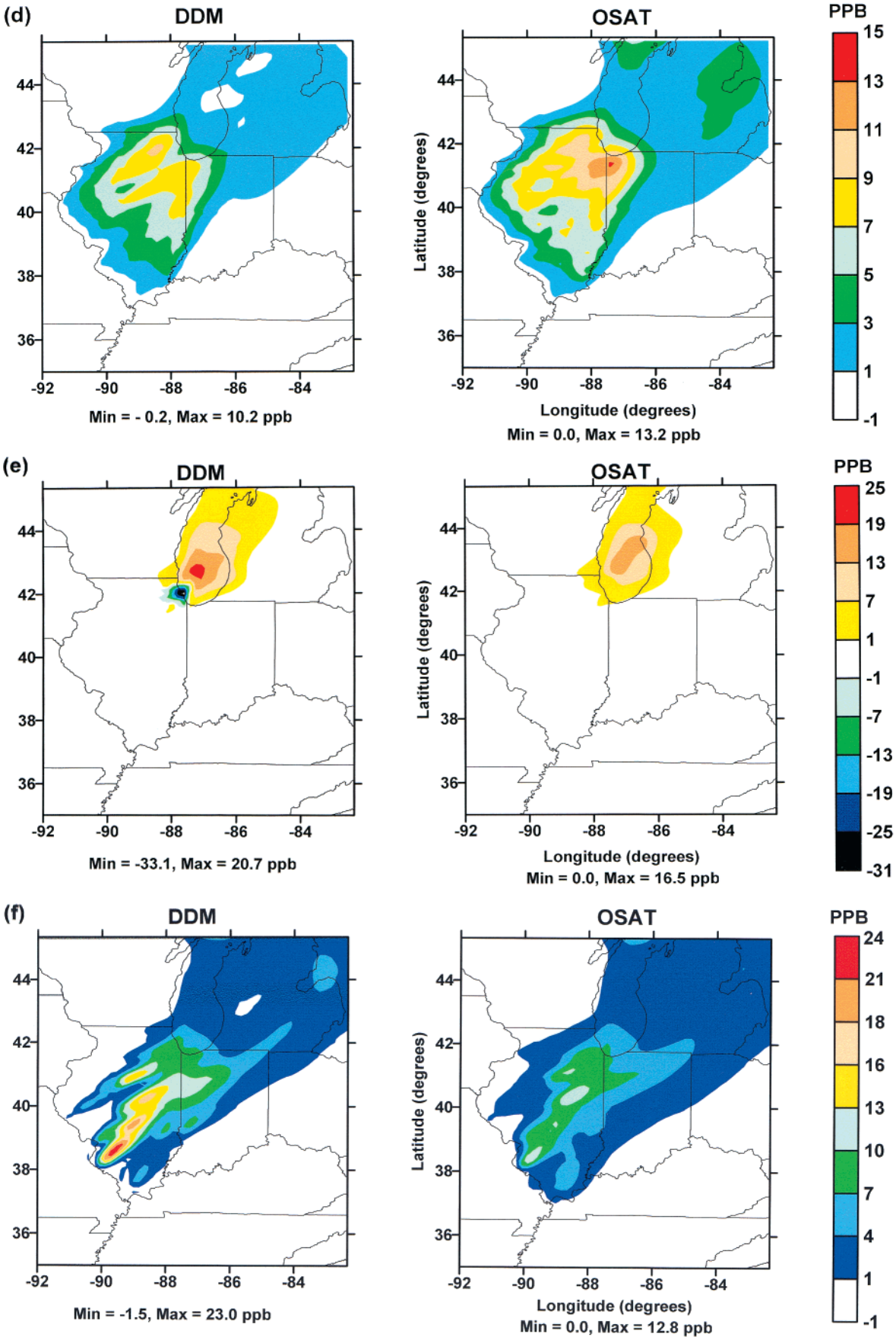

FIGURE 5. (Continued) (c) point-source VOC emissions from source region 3; (d) biogenic NO_x emissions from source region 6; (e) anthropogenic area-source NO_x emissions from source region 3; (f) point-source NO_x emissions from source region 6.

indicate a clear disagreement between DDM and OSAT. In particular, slopes greater than 1.0 indicate a strong disagreement because the general tendency is for the sensitivities to be smaller than the source contributions. Taking into account this tendency, there remains disagreement between the DDM and OSAT results for area-source NO_x emissions and boundary VOC and NO_x concentrations and strong disagreement for area-source VOC emissions and point-source VOC and NO_x emissions.

Another source of the disagreement between DDM and OSAT arises from allocating the net ozone change in eqs 6 and 7, rather than allocating the ozone production and the ozone destruction separately. At the beginning of a time step, ozone is normally present due to production in earlier time steps from upwind emissions and due to the ozone BCs. Some of this preexisting ozone is then destroyed over the time step by various reactions (e.g. $O_3 + HO_x$, O_3 + VOCs, $O_3 + h\nu \rightarrow O^1D$). Simultaneously, new ozone is generated via various routes involving VOCs, NO_x, and HO_x. Equations 6 and 7 are used only when there is net ozone production, but this net production may include both large production and destruction terms. Further, the ozone production is approximately proportional to the N_i or $k\mathrm{OH}_i \times V_i$ tracers, but the ozone destruction is proportional to the $O3N_i$ and $O3V_i$ tracers. Because eqs 6 and 7 use only the N_i or $k\mathrm{OH}_i \times V_i$ tracers, there is an implicit assumption that the ozone destruction is small. If the ozone destruction is large, the net ozone production is allocated in such a way that the lifetime of the preexisting ozone is lengthened.

Consequently, the influence of the ozone BCs extends further into the domain with OSAT than DDM, especially during the daytime when the $O_3 + HO_x$ and $O_3 + h\nu \rightarrow O^1D$ reactions are important. We tested improvements to OSAT that allocate ozone production and destruction separately when there is net ozone production, and these changes greatly reduce, but do not eliminate, this difference between DDM and OSAT. The difference in range of influence seen for ozone BCs likely also applies to ozone generated from emissions within the modeling domain, whenever there is predominantly net ozone production. Also, if there is net ozone destruction due to the $O_3 + NO$ reaction, OSAT allocates this destruction to both the $O3N_i$ and $O3V_i$ tracers (eq 8 and the analogous equation for $O3V_i$). This may cause some differences between DDM and OSAT because DDM ascribes such ozone destruction solely to the NO emissions.

A third source of the disagreement between DDM and OSAT is probably the PAN BCs. The sensitivity to the PAN BCs is about 25% of the sensitivity to all other BCs combined, but the sensitivity to PAN is not included in the DDM results in Figure 4, parts d and h, because OSAT does not track PAN explicitly. However, the ozone generated from the PAN BCs is allocated implicitly to other source contributions in OSAT and appears in the OSAT results in one or more plots of Figure 4a−h.

Last, the reactivity weighting used in OSAT likely accounts for some of the differences with the DDM results. The reactivity weighting is based on OH reaction rates, but this represents only the initial step in the VOC chemistry. The DDM sensitivities include effects of the complete chemistry. The differences for VOC emissions and BCs, Figure 4a−d, may be a consequence, in part, of the simplified reactivity weighting used in OSAT. A more comprehensive approach used in developing reactivity scales is to view the total reactivity as the product of kinetic and mechanistic components (*16*). The OSAT might be improved by using the kinetic reactivity $k\mathrm{OH}_i$ in eq 5, because VOC decay is closely related to OH attack, but a total reactivity, such as the maximum incremental reactivity (*16*), in eq 7 to account for more of the chemistry in ozone formation.

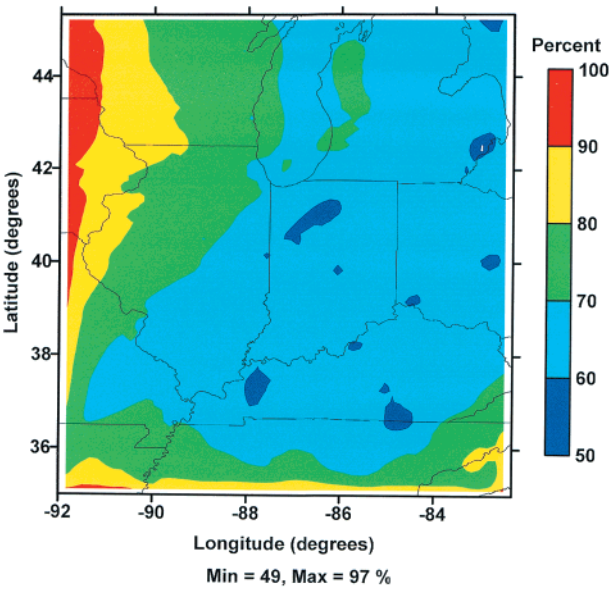

FIGURE 6. Sum of the sensitivities of ozone to emissions and boundary and initial concentrations as a percent of the ozone concentration on July 13, 1995, 1500−1600 CST.

Comparison of Spatial Distributions. We also compared the spatial distributions of the sensitivities and source contributions for the different emission categories, source regions, and boundaries. Figure 5 contains typical results for emissions from source regions 3 (Chicago area) and 6 (remainder of Illinois) on July 13, 1995, 1500−1600 CST. While Figures 3 and 4 focus on the receptor regions and grid cells with ozone > 80 ppb, Figure 5 focuses on all grid cells, regardless of location or ozone concentration.

The spatial distributions of the sensitivities and source contributions are similar in all cases. Also, the maximum (positive) values for OSAT and DDM occur in the same location, as in Figure 5, parts a−c, e, and f, or relatively nearby locations, as in Figure 5d. The minimum (negative) sensitivity values at this hour are in the range 0.0 to −1.5 ppb, with the exception of the sensitivity to anthropogenic area-source NO_x emissions, Figure 5e, for which the minimum is −33 ppb. In the region of this large negative sensitivity, the OSAT source contribution is 0.3−2.6 ppb.

The relative magnitudes of the sensitivities and source contributions in Figure 5 are generally in agreement with the results in Figure 4. However, Figure 5a suggests more strongly than Figure 4a that the source contributions are larger than the sensitivities for biogenic VOC emissions. Similarly, Figure 5, parts e and f, indicate more strongly than Figure 4, parts f and g, that the sensitivities are larger than the source contributions for area-source and point-source NO_x emissions.

Sum of Sensitivities. As seen from eq 12, the sum of all of the first-order sensitivities is a measure of the degree to which these sensitivities explain the ozone concentration. Also, the difference between the ozone concentration and the sum of the first-order sensitivities is a measure of the importance of the second- and higher-order sensitivities. Within our implementation of the DDM (*4*, *6*), we easily obtained the sum of all the first-order sensitivities by calculating and adding just three sensitivities: the sensitivity to all emissions, the sensitivity to all BCs, and the sensitivity to all ICs. Each sensitivity incorporates the sensitivity to all species, including PAN and CO. Figure 6 gives the sum of the first-order sensitivities as a percentage of the ozone concentration over the entire modeling domain on July 13, 1995, 1500−1600 CST.

TABLE 2. CPU Time for DDM and OSAT Simulations on July 7 with 12 km Grid

tool	number of inputs studied[a]	total time (min)[b]	time per input[c]
DDM	0[d]	37.0	
	24	406.3	0.42
	42	667.5	0.41
OSAT	90	140.2	0.03

[a] Emissions, boundary concentrations, and/or initial concentrations. [b] Sun Ultra 60 workstation, 360 MHz processor. [c] Normalized to time required for concentrations only: $[T(n) - T(0)]/nT(0)$ where $T(n)$ is the total time to calculate the concentrations and results for n inputs. [d] Concentrations only.

Over much of the domain, the sum of the sensitivities is 60−70% of the ozone concentration. This rises to 97% along the west and south boundaries, which at 1500−1600 CST are the inflow boundaries. There are a few small areas in which the sum is 50−60% of the ozone concentration. Interestingly, the sum is always <100% of the ozone; thus, the net contribution of all of the higher-order sensitivities in eq 12 is positive. Averaged over the entire domain, the sum of the first-order sensitivities is 71% of the ozone concentration. This is higher than expected, considering that only first-order sensitivities are included in the sum and that the sensitivities are calculated using the full emissions, ICs, and BCs (i.e., $\lambda_j = 0$ in eq 11). In essence, the sum of the first-order sensitivities is an extrapolation of the ozone concentration from $\lambda_j = 0$ to $\lambda_j = -1$. For extrapolation over such a wide range, simulations with a box model (*17*) suggest that the higher-order sensitivities would be more important than indicated by Figure 6.

Efficiency. Table 2 gives a comparison of the CPU times for DDM and OSAT. If the incremental time required to calculate a sensitivity or source contribution is normalized by the time required to calculate the concentrations alone, then the time per input is a factor of ∼14 less for OSAT than DDM (0.03 vs 0.41). (Here, an input is one of the 90 contributors to ozone considered by OSAT (e.g., NO_x emissions from point sources in source region 6).) The difference in efficiency is due to two factors. First, OSAT provides results for three species or species groups (ozone, total NO_x, and total VOCs), whereas DDM provides results for the 25 species in the CB IV mechanism that are transported between grid cells. Thus, there is a difference of about a factor of 8 in the amount of information generated. Second, OSAT uses the chemical information available from calculating the concentrations, whereas DDM solves additional chemistry-related equations. These additional equations follow the first-order impact of the input changes through all 37 species in the CB IV mechanism, and solution of the equations requires ∼60% of the CPU time for the DDM. Hence, the additional equations account for a factor of ∼2 of the difference in efficiency.

Advantages and Limitations. The OSAT has the advantage of being relatively simple but yet providing a distinction between the contributions of VOC and NO_x emissions to ozone. Another advantage is that the ozone is allocated to emissions, ICs, and BCs such that the sum of the individual allocations is the total ozone concentration. Also, the OSAT requires substantially less computer time than the DDM for the same subdivision of the model inputs (i.e., same number of emission categories and geographic regions).

One limitation of OSAT is that ozone destruction mechanisms are not explicitly separated from ozone production, which tends to overestimate the area of influence of ozone from a particular source. Also, some ozone precursors are not tracked, most importantly the CO emissions and PAN BCs. Ozone from these precursors is implicitly allocated to other emissions or BCs. In addition, the ozone BCs are not tracked separately but included with the VOC and NO_x BCs. (These limitations could likely be removed by adding additional tracers.) Using the average OH reactivity to apportion ozone formation from VOCs is an approximation that becomes less accurate as the range of reactivity widens. A practical approach to minimizing this limitation is to separately track emission categories or geographic regions with widely disparate VOC reactivity (e.g., biogenic VOC emissions should be considered separately from most anthropogenic VOC emissions). The OSAT also has the two limitations of all source apportionment techniques, namely, the apportionment is not unique and there is no mathematical relationship between the apportionment and the response to input changes.

First-order sensitivities have the advantage of being related mathematically to the governing equations for the concentrations. No additional assumptions are necessary regarding the reactivity of VOCs or when the chemistry is VOC- or NO_x-sensitive. A second advantage is that the sensitivities describe both positive and negative impacts on ozone, which is important in some cases where reducing emissions can increase ozone and vice versa. Third, the number of parameters λ_j for which sensitivities are calculated and the geographic size of the emission regions is arbitrary. Thus, sensitivities can be calculated for only a subset of the emission sources, if only these sensitivities are needed. Last, calculating the sensitivities by the DDM gives information on the sensitivity of all species, not just ozone, to the model inputs.

One limitation of first-order sensitivities is that they describe the impact of input changes on ozone less accurately as the magnitude of the changes increases, due to the importance of the higher-order, nonlinear terms in the Taylor series (*4*). Consequently, the sum of all of the first-order sensitivities will not equal the ozone concentration (eq 12). Also, the nonlinear terms likely vary in importance for different emission sources and BCs. The other major limitation is the greater computer time required for the DDM compared to the OSAT. This is offset, in part, by the ability to define larger source groups with the DDM (regardless of reactivity differences among the sources) and to include only those source groups of interest.

Different procedures for source apportionment will very likely produce different results because there is no unique source apportionment (as indicated in the Introduction). Rather than compare OSAT to a different procedure for source apportionment, we compared OSAT to a different tool, sensitivity analysis. This allowed us to determine the accuracy of the source contributions for the purpose of predicting the effects of input changes. The DDM sensitivities were found to predict quite accurately the ozone changes corresponding to reductions of up to ∼40% in emissions, ICs, and BCs (*4*). Hence, the OSAT results should be used with caution in predicting the absolute or relative impact of small to moderate changes in model inputs. In such applications, the OSAT results may overestimate the importance of the BCs and underestimate the importance of the anthropogenic emissions, based on the comparisons in Figures 4 and 5.

Acknowledgments

The authors gratefully acknowledge the support of the Coordinating Research Council under Project A-29 and the additional support provided by ENVIRON International Corp. and the General Motors R&D Center.

Literature Cited

(1) Dunker, A. M.; Morris, R. E.; Pollack, A. K.; Schleyer, C. H.; Yarwood, G. *Environ. Sci. Technol.* **1996**, *30*, 787−801.
(2) Dunker, A. M. *Atmos. Environ.* **1981**, *15*, 1155−1161.

(3) Yang, Y.-J.; Wilkinson, J. G.; Russell, A. G. *Environ. Sci. Technol.* **1997**, *31*, 2859−2868.
(4) Dunker, A. M.; Yarwood, G.; Ortmann, J. P.; Wilson, G. M. The Decoupled Direct Method for Sensitivity Analysis in a Three-Dimensional Air Quality Model—Implementation, Accuracy and Efficiency. *Environ. Sci. Technol.* **2002**, in press.
(5) Yarwood, G.; Morris, R. E.; Yocke, M. A.; Hogo, H.; Chico T. *Proceedings of the 89th Annual Meeting of the Air & Waste Management Association*; Air and Waste Management Association: Pittsburgh, PA, 1996; Paper 96-TA23A.06.
(6) *User's Guide—Comprehensive Air Quality Model with Extensions (CAMx), version 3.00*; Environ International Corp.: Novato, CA, Dec, 2000.
(7) Yarwood, G.; Morris, R.; Emery, C.; Wilson, G. *Proceedings of the 91st Annual Meeting of the Air and Waste Management Association*; Air and Waste Management Association: Pittsburgh, PA, 1998; Paper 98-MP2B.06.
(8) CAMx v. 3.00 with the DDM for sensitivity analysis, OSAT and other features is available at http://www.camx.com.
(9) Smolarkiewicz, P. K. *Mon. Wea. Rev.* **1983**, *111*, 479−486.
(10) Colella, P.; Woodward, P. R. *J. Comput. Phys.* **1984**, *54*, 174−201.
(11) Bott, A. *Mon. Wea. Rev.* **1989**, *117*, 1006−1015.
(12) Sillman, S. *J. Geophys. Res.* **1995**, *100*, 14175−14188.
(13) Gery, M. W.; Whitten, G. Z.; Killus, J. P.; Dodge, M. C. *J. Geophys. Res.* **1989**, *94*, 12925−12956.
(14) Carter, W. P. L. *Atmos. Environ.* **1996**, *30*, 4275−4290.
(15) *Midwest Subregional Modeling: Analysis of NOx SIP Call*; Illinois Environmental Protection Agency, Indiana Department of Environmental Management, Michigan Department of Environmental Quality, Wisconsin Department of Natural Resources: Chicago, IL, March, 1999.
(16) Carter, W. P. L.; Atkinson, R. *Environ. Sci. Technol.* **1989**, *23*, 864−880.
(17) Vuilleumier, L.; Harley, R. A.; Brown, N. J. *Environ. Sci. Technol.* **1997**, *31*, 1206−1217.

Received for review November 13, 2001. Revised manuscript received April 15, 2002. Accepted April 22, 2002.

ES011418F